

## COMPARISON OF MECHANICAL PROPERTIES OF CFRP LAMINATE OBTAINED FROM FULL-SCALE TEST AND EXTRAPOLATED FROM LOCAL MEASUREMENT

JAROSLAV VALACH<sup>a\*</sup>, DANIEL KYTÝŘ<sup>a</sup>,  
TOMÁŠ DOKTOR<sup>a</sup>, KLÁRA SEKYROVÁ<sup>a</sup>,  
VLASTIMIL KRÁLÍK<sup>b</sup>, and JIŘÍ  
NĚMEČEK<sup>b</sup>

<sup>a</sup> Czech Technical University in Prague, Faculty of Transportation Sciences, Na Florenci 25, 110 00 Prague 1, <sup>b</sup> Czech Technical University in Prague, Faculty of Civil Engineering, Thákurova 7, 166 29 Prague 6  
valach@fd.cvut.cz

Keywords: CRFP laminate, fatigue test, nanoindentation

### 1. Introduction

Since from the very beginning of aviation, the research was focused on lightweight and strong materials. Due to continuous research and investment, various novel materials successfully compete with once dominating light metal alloys. In comparison with metals, composites offer favorable strength to density and stiffness to density ratios and also superior fracture toughness properties implied by nature of their micro-structure. However, the behavior of the applied materials is sufficiently known to be operated safely in civil aircraft, a complete understanding of these materials is yet to be built. One example supporting this statement are difficulties in generalization of observations and tests of the materials' degradation properties. The difficulties arise from composites heterogeneity, engaging several damage mechanisms acting at several scales and also from the long-time experiments necessary for study of materials' degradation processes.

The research presented in this paper is a part of an extensive investigation of the fatigue behavior of the special class of carbon fibre reinforced plastics (CFRP) represented by carbon fibre in polyphenylene sulfide thermoplastics matrix (C/PPS) composites used in the aircraft industry.

The main aim of the paper is to show correlation between decrease of the material's stiffness during cyclic loading and the associated changes in the matrix properties.

### 2. Problem and material overview

From the technical point of view the material's degradation due to external loading ultimately manifests itself in the decrease of the strength. As this property cannot be determined nondestructively, other mechanical properties of the materials, are used as damage indicators<sup>1</sup>. Prominent role among these indicators is assigned to the measurement of modulus of elasticity: damage accumulation causes weakening of the material's internal bonds and increase of its compliance or, equivalently, decrease of its stiffness<sup>2</sup>.

The concepts, as classified e.g. in a review paper<sup>3</sup>, can be divided into the three groups: fatigue life investigation, residual stiffness determination and damage accumulation mea-

surement. The first one constructs S-N curve relating strength to the number of cycles, but ignoring detailed model of the damage process in the material, this approach does not discriminate between fatigue of metals and other materials, however it is obvious that underlying mechanisms differ fundamentally. The second approach builds criteria based upon phenomenological description of the remaining strength or stiffness; it is considered the most suitable for experimental investigation as it yields nondestructively measurable property. Finally, the third approach studies a detectable property of material directly associated with damage accumulation from micromechanical viewpoint. According to the above mentioned classification, the presented results intend to demonstrate a connection between residual stiffness and damage mechanism.

The C/PPS composite is a relatively new material; it is quasi-isotropic 8-ply of carbon fabric bonded by thermoplastic matrix, a notable difference from more common composites based on epoxy resin. Its modulus to weight and strength to weight ratios favors this material for hi-tech application. The composite under investigation contains the carbon fibers prepared from PAN (Poly acrylonitrile), which are among those of the highest stiffness from the range from 40 to 400 GPa known from literature<sup>4-6</sup>. The reasons for this striking variation are different manufacturing methods adopted by industry. In contrast to glass fibres the carbon ones are highly anisotropic and design of composite takes often an advantage from this fact. Further details of mechanical and other properties can be found in materials datasheets<sup>7</sup>.

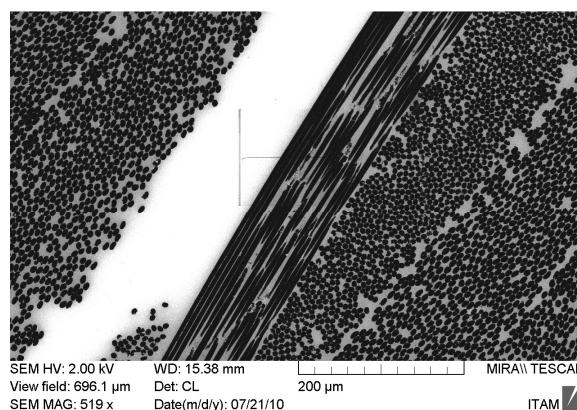


Fig. 1. SEM micrograph of CFRP taken in CL regime depicts in high contrast density of fibers in various plies as well as their orientation. Ellipses of cross section of the fibers indicate the angle of cut in relation to axis of fibre

### 3. Experimental procedure

The experiments were carried out on typical tensile specimen (depicted in cross section in Fig. 1 and in overall view

in Fig. 2) with rectangular cross-section 25×2.5 mm and total length 250 mm. For the fatigue testing servo-hydraulic Instron 1603 loading machine was used. The outputs of the force and displacement transducers were captured with 10 Hz sampling frequency. A sinusoidal force with 3 Hz frequency was applied. According to chosen stress level (76 % of limit tensile strength) mean loading force value (13 kN) and amplitude (12 kN) were set up. Fatigue experiment was six times interrupted at predefined intervals and number of cycles in order to determine damage indicators, i.e. to measure the stiffness.

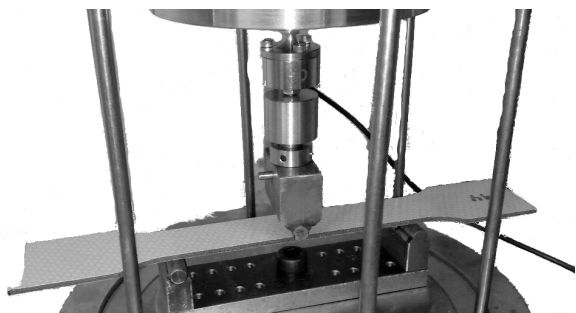


Fig. 2. Three point bending testing device

The stiffness was determined using three point bending (3PB) and from the ultrasound (US) measurement. Although different physical principles are involved in the both methods for elastic modulus determination, the results are very close for the intact specimens.

The experiment was carried out using testing device USG 20 (Krompholz Geotron Elektronik, FRG) used with a 250 kHz transducer (USG-T) and receiver (USE-T). The velocity of the longitudinal ultrasonic waves' propagation depends on the mechanical properties of the material, therefore the Young's modulus can be obtained from the formula for coupling elasticity modulus  $E_{ad}$

$$E_{ad} = \rho v^2$$

in which,  $v$  stands for the wave velocity and  $\rho$  is the material density.

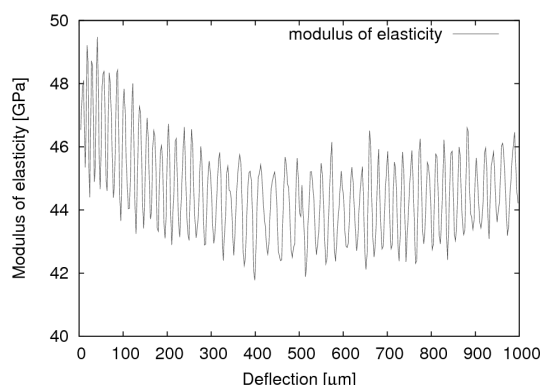


Fig. 3. Values of Young's modulus during the 3PB test

Three point bending measurements were performed using an uniaxial loading device as shown in Fig. 2. The loading run was controlled by displacement with maximal deflection value 1000 µm. The support span was 120 mm. The Young's modulus was calculated using the incremental method. Fig. 3 shows values of Young's modulus acquired in 3PB test. The values corresponding to deflections 0 to 100 µm were excluded because of settlement of the experimental setup.

#### 4. Nanoindentation

Nanoindentation plays a unique role in the presented investigation due to its ability to distinguish between fibres and matrix and to measure these properties separately. Considering the components' properties evolution, their contribution to the composite degradation can be estimated to identify the primary cause of breakdown.

The nanoindentation was carried out on the intact specimen and on the ruptured one (indicated in Fig. 4).

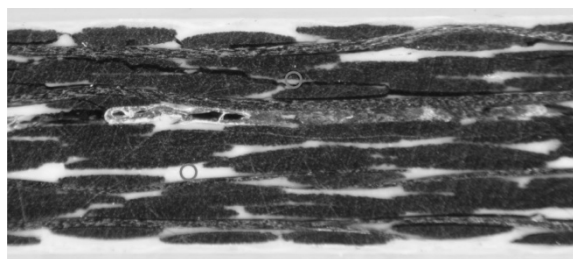


Fig. 4. Polished surface from the ruptured specimen. A production imperfection is clearly visible. During rupture the delamination cracks were created, some of them are clearly visible above the inclusion. Location of nano indentation are marked by circles

To conform nanoindentation requirements, the cross section surface was carefully polished to provide desired flatness and smoothness. Scanning Probe Microscopy (SPM) was used to obtain the information about the surface roughness before testing. Achieved value of the surface roughness was 30 nm or less.

For the tests, Hysitron TriboIndenter Ti750 (Hysitron, Inc.) with Berkovich tip diamond indenter (three-sided pyramid) was used. The duration of the loading phase was 5 s and the maximum loading force 1000 µN was kept for 10 s. The duration of the unloading phase lasted for 5 s. Twenty five indents were performed in a 5×5 grid. Comparison of nanoindentation loading curves of intact and ruptured specimen is shown in Fig. 5.

The nanoindentation into carbon fiber yields the results of  $E=18$  GPa in the longitudinal cross section and  $E=25$  GPa in the transversal cross section. The difference between these values can be explained by the effect of internal fiber structure and compliant matrix that surrounds relatively stiff and elastic fibers. The carbon fibre can be imagined as a bundle of narrow carbon (graphite) ribbons that rearrange easily during the penetration of indenter.

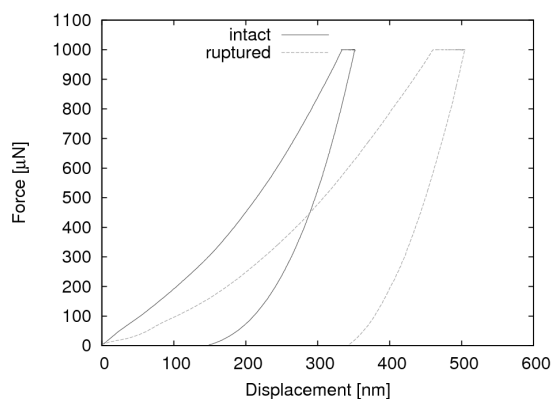


Fig. 5. Nanoindentation loading curves

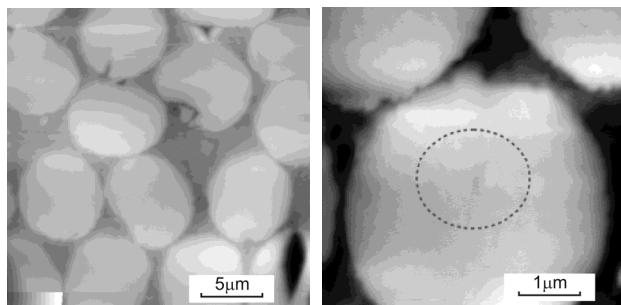


Fig. 6. Nanoindentation of fibres in the transversal cross section

This behavior also clarifies the observed fact that nanoindenter tool does not leave any traces on carbon fiber (see Fig. 5). Indents in the matrix were clearly visible, therefore the nanoindentation tests of the matrix were used for the observation of the degradation process.

## 5. Results

The fatigue testing was terminated after 789,183 cycles when the specimen was ruptured. The degradation of the Young's modulus during the cyclic loading is depicted in Fig. 7 and listed in Tab. I.

Comparing two macro-mechanical measurements, the following observations were made: values of the adiabatical modulus of elasticity remain at various stages of the fatigue test within the range of measurement error the same, while the stiffness derived from flexure test decreases.

The decrease in stiffness values as measured by the 3PB test and the fact of different values obtained by the US tests are caused by different physical background of the used measurement techniques. The dynamic modulus of elasticity depends on the pressure wave velocity in material. This principle naturally suppresses the influence of many defects, as it tends to close cracks and detour broken fibers. In contrast with this measurement, the bending tests “activates” defects on the strained side of the specimen, exposing hidden faults.

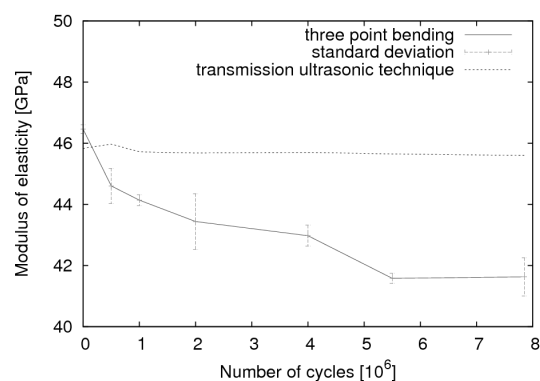


Fig. 7. Comparison of static and dynamic moduli of elasticity evolution in fatigue testing

Table I

Comparison of the Young's modulus decrease obtained by different techniques

Technique/Young's modulus [GPa]	Intact specimen	Ruptured specimen
Overall properties		
Ultrasound	45.83	45.61
Three point bending	46.46	41.63
Matrix properties		
Nanoindentation	5.63	4.09

The stiffness' invariability in US measurement reveals fully elastic behavior and integrity of carbon fibres and their bonds to the matrix. The lack of broken fibres and delamination points toward the properties of the matrix accounting for the damage accumulation as the only component that can deteriorate and be responsible for the flexural stiffness decrease. Micromechanically, the matrix transfers loads across the volume of the composite. Shear compliance of the matrix as a softer component of the composite is responsible for the shear properties of the whole composite. This hypothesis was verified by matrix nanoindentation in the beginning and in the end of the fatigue test.

## 6. Discussion and conclusions

Successful comparison of macro- and micro- measurement presented in this paper brings in a hope of more fundamental understanding of the processes during fatigue loading. Obtained results couple nondestructively measurable damage indicators with the changes in microstructure and component's properties. The measurement proved prominent role of the matrix in the composite's properties fatigue degradation.

The presented study describes the possibility of assessment of the fatigue behavior using the micromechanical testing. But the problems that occurred show on some limitations of used techniques. For more complex description of the dis-

tinct components in the composite material, nanoindentation and microtensile tests of separated phases can be helpful.

*The research has been supported by Grant Agency of the Czech Technical University in Prague (grants No. SGS10/218/OHK2/2T/16, SGS10/135/OHK1/2T/11), by the Grant Agency of the Academy of Sciences (grant No. IAA200710801) and by research plan of the Ministry of Education, Youth and Sports MSM6840770043.*

#### REFERENCES

1. Van Paepegem W., De Baere I., Lamkanfi E., Degrieck J.: *Poisson's ratio as a sensitive indicator of (fatigue) damage in fibre-reinforced plastics*, Fatigue & Fracture of Engineering Materials & Structures 30(4), 269–276, Wiley Online Library, 2007.
2. Vasiliev V. V., Morozov E. V.: *Mechanics and analysis of composite material*, Elsevier (2001).
3. Degrieck J., Van Paepegem W.: Appl. Mech. Rev. 54, 279 (2001).
4. Maurin R., Davies P., Baral N., Baley C.: Appl. Compos. Mater. 15, 61 (2008).
5. Kriz R. D., Stinchcomb W. W.: Exp. Mech. 19, 41 (1979).
6. Kelly A.: Compos. Sci. Technol. 65, 2285 (2005).
7. Airbus: *AIMS - Airbus Material Specification*, Airbus S.A.S (2007).

**J. Valach<sup>a</sup>, D. Kytýř<sup>a</sup>, T. Doktor<sup>a</sup>, K. Sekyrová<sup>a</sup>, V. Králík<sup>b</sup>, and J. Němeček<sup>b</sup>**, (<sup>a</sup> *Czech Technical University in Prague, Faculty of Transportation Science, Prague*, <sup>b</sup> *Czech Technical University in Prague, Faculty of Civil Engineering, Prague, Czech Republic*): **Comparison of Mechanical Properties of CFRP Laminate Obtained from Full-Scale Test and Extrapolated from Local Measurement**

The presented paper outlines experimental investigation that is a part of an extensive research plan of study of fatigue properties of aerospace industry grade CRFP laminates. These materials are relatively novel and their long-term behavior and degradation are not yet completely described. Deterioration of this complex material in cyclic loading conditions is to be evaluated by several criteria based on evolution of certain of mechanical properties. Among the criteria is a decrease of modulus of elasticity. In order to reliably detect the changes in this property sensitive three point bending experimental setup was prepared, calibrated and compared to the results of the independent ultrasound method yielding the dynamical modulus of elasticity. Simultaneously, the local mechanical properties were studied by nanoindentation in order to set a reference point for a successive measurement after fatigue tests.

## 3D REPLICATION OF SURFACE STRUCTURES BY RAPID PROTOTYPING TECHNIQUE

**VLADIMÍR PATA\***, **MIROSLAV MAŇAS**,  
**DAVID MAŇAS**, and **MICHAL STANĚK**

*Tomas Bata University in Zlin, Nam. T. G. Masaryka 5555,  
760 01 Zlin, Czech Republic  
pata@ft.utb.cz*

Keywords: Surface structure, replication, rapid prototyping

### 1. Introduction

The replication of surface structures is a process which can be widely applied for the assessment of the surface quality of technical components made from metal and polymer material from the point of visualization<sup>1,2</sup>.

There are a number of manufacturers focusing on the production of single purpose machines which scan and then assess the surface quality according to the relevant ISO standards in both 2D and 3D. The result is either numerical parameters of the surface quality or special graphs, which can, however, be very difficult to interpret for a user who does not specialize in the assessment of the surface quality. It is also necessary to take into account the fact that it is rather complicated to achieve the same conditions for reproducibility of measurements of the surface quality. Visualization of the scanned surface is at present only possible by using single purpose programmes supplied together with the machine which, however, lack compatibility with each other.

#### 1.1. Surface mask

The principle of 3D replications of surface structure of the specimen structure is using 3D scanner with the defined step in axis *x* and *y*. The specimen used for surface replication is covered by a mask made from thin elastic material, which has a hole of rectangular shape whose edges correspond with the size of the scanned surface – see Fig. 1.

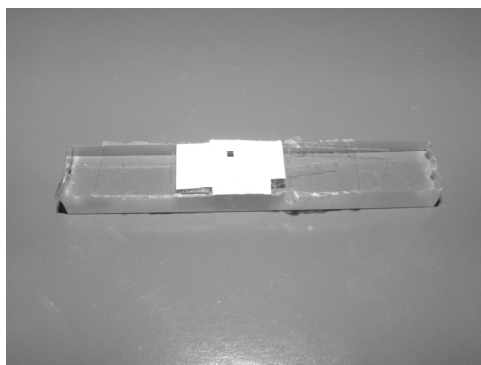


Fig. 1. Specimen with applied mask

#### 1.2. Technique for scanning the surface coordinates

The next step is to scan the coordinates of the surface using the three dimensional matrix *x,y,z*. This matrix is then exported through ASCII file and adjusted by single-purpose programme for rapid prototyping process, in which we obtain the required replication of the scanned surface structure at a selected scale. Besides rapid prototyping technique it is also possible to use the import of the data adjusted as above into a CAD programme, generate automatically the relevant tool paths and make the replication of the surface structure using a CNC milling machine. The size of the replicated surface is limited only by the parameters of rapid prototyping, or the CNC milling machine.

### 2. Examples of practical applications

The applicability of the above mentioned process of surface structure replication was confirmed on one example in which microhardness of a specimen made from polymethylmetacrylate, commercially known as Plexiglass, is measured and assessed. After the measurement of microhardness the tested specimen shows an imprint of a pyramid. The diagonals of the pyramid are 0.020 mm and its height 0.015 mm. Because of relaxation of the specimen material the imprint is deformed, which needs to be visualized and then assessed. The methods used so far could be visualized only by using an electron microscope, e.g. SEM. When the surface was covered by a mask made from paper with a hole in the shape of a square of 0.6 mm, the surface was scanned by 3D scanner of Taylor Hobson with a CLA scanner with a step in axis *x* and *y* 0.0005 mm. After the scan, the three dimensional matrix of coordinates was transferred to the above mentioned single-purpose programme and then adjusted for 3D print using the rapid prototyping technique.

Fig. 2 shows a surface visualized in 3D using the commercial programme Talymap of Taylor Hobson and Fig. 3 shows the replication of the surface of the specimen with the imprint after the relaxation.

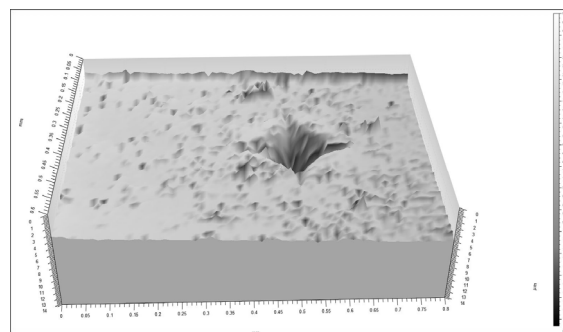


Fig. 2. The surface of the specimen made by Talymap programme



Fig. 3. Replication of the specimen surface using the rapid prototyping technique

Fig. 4 shows 3D image of the structure of a specimen made from steel 12020, which was machined by face milling technique. The size of the scanned surface is 4 mm × 2 mm. Fig. 5 is its 3D replication made by the same technological process.

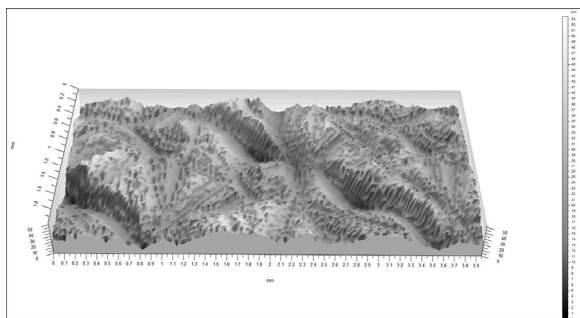


Fig. 4. 3D image of the specimen surface made by Talymap programme



Fig. 5. 3D replication of the surface structure of the specimen created by rapid prototyping technique

### 3. Conclusion

The process of replication of surface structures described above is very suitable in the instances when it is necessary to make 3D replication of the assessed surface, which is mainly interesting from the tribological point of view.

Next, it is possible to replicate different defects at a selected scale which occur on the surface of specimens and lower its quality, such as scratches, cracks, fissures, etc. This is very useful in the field of "Forensic Engineering"<sup>3-5</sup>. Using 3D replication helps to visualize defects, which are on the specimen, and hence it is not necessary to use special projection or photo documentary techniques.

*This article is supported by the European Regional V & V center in the project CEBIA – Tech, no. CZ. 1. 05/2. 1. 00/03. 0089 and the internal grant of TBU in Zlin No. IGA/10FT/11//D funded from the resources of specific university research.*

### REFERENCES

1. Manas D., Manas M., Stanek, M., Pata V.: Wear of Tire Treads. *Archives of Materials Science* Volume 28 (1–4), 2007 Pages 81 – 89, Committee of Materials Science of the Polish Academy of Sciences, Warszawa, Poland.
2. Manas D., Stanek M., Manas M., Pata V., Javorik J.: KGK, *Kautsch. Gummi Kunstst.* 62, 240 (2009).
3. Manas D., Manas M., Stanek M., Zaludek M., Sanda S., Javorik J., Pata V.: *Chem. Listy* 103, 72 (2009).
4. Manas D., Manas M., Stanek M., Pata V.: *International Rubber Conference – IRC 2008*, 20 – 23.10.2008, Kuala Lumpur, Malaysia, p.37–48.
5. Manas D., Pata V., Manas M., Stanek M.: *8<sup>th</sup> Fall Rubber Colloquium 2008, Hannover*, 26 – 28.11.2008, Germany, p.93–94.

**V. Pata, M. Mañas, D. Mañas, and M. Staněk** (*Tomas Bata University in Zlin, Zlin, Czech Republic*): **3D Replication of Surface Structures by Rapid Prototyping Technique**

The article describes the possibilities of 3D replications of surface structures by the rapid prototyping technique. It presents the method of masking the surface of the specimen in order to make the scanning of the required structure more precise. Next, it describes the method of scanning and assessing the data through the surface matrix. Finally, the above is documented by 3D replications of a specimen made from "polymethylmetacrylate" which was used for the assessment of microhardness, and a specimen from steel 12020 machined by the face milling technique.

## USE OF THE INDENTATION TESTS FOR THE EVALUATION OF MACHINABILITY OF MATERIALS DURING ABRASIVE WATERJET CUTTING

**PETR HLAVÁČEK<sup>a,\*</sup>, JAN VALÍČEK<sup>a</sup>, JAN BRUMEK<sup>b</sup>, MICHAL ZELENÁK<sup>a</sup>, BARBORA HALUZÍKOVÁ<sup>a</sup>, MARTA HARNIČÁROVÁ<sup>c</sup>, and VERONIKA SZARKOVÁ<sup>d</sup>**

<sup>a</sup>Institute of Physics, Faculty of Mining and Geology, VŠB-TUO, 17. listopadu, 708 33 Ostrava - Poruba, Czech Republic; <sup>b</sup>SMID - CPIT, VŠB - TUO, 17. listopadu, 708 33 Ostrava - Poruba, Czech Republic; <sup>c</sup>Faculty of Manufacturing Technologies of Technical University of Košice with a seat in Prešov, Bayerova 1, 080 01 Prešov, Slovak Republic; <sup>d</sup>Institute of Economics and control systems, Faculty of Mining and Geology, VŠB - TUO, 17. listopadu, 708 33 Ostrava - Poruba, Czech Republic  
petr.hlavacek@vsb.cz

Keywords: hydroabrasive erosion, machinability, instrumented indentation test

### 1. Introduction

The hydroabrasive machining is a technological process which used a high pressure waterjet with addition of abrasive material with a purpose of a controlled abrasive action. It is used to cut almost any material. The hydroabrasive machining can be carried out either by a suspension abrasive waterjet (Abrasive Slurry Jet – ASJ) or more often by an abrasive waterjet (Abrasive Water Jet – AWJ)<sup>1</sup>. In this work the experiments were performed by the AWJ technology, but a proposed methodology for the materials machinability can be generalized and used also in the ASJ technology.

The AWJ is used to accelerate the abrasive particles (mostly garnet) for disintegration of materials. The abrasive waterjet has many outstanding features that make it ideal for use in a wide range of applications. There is no heat affected zone during the abrasive waterjet machining (the maximum temperature of cut is about 70 °C). This feature is used for example to secure the disposal of munitions<sup>2</sup>. Very low cutting forces (below 50 N) affect the process of machining, so that mechanical stresses do not arise and also there are no residual stresses within the machined material<sup>3</sup>.

### 2. Evaluation of the materials machinability

The term machinability is used for the cumulative effects of physical properties and chemical composition of materials on the process flow and economic or qualitative results of the machining process. The machinability generally can be considered in terms of an impact of material on the intensity of tool wear, energy balance of the cutting process and their effects on the chip and new surface formation within the conventional machining technologies. Knowledge of the machin-

ability can be used for prediction, control and optimization of technological parameters of the machining process.

Current state of the evaluation of the materials machinability in the AWJ technology

For the evaluation of the materials machinability in the abrasive waterjet technology, there are many models for prediction, control and optimization<sup>5–8</sup>. Hashish was one of the first pioneers in this field, who has proposed a comprehensive model for prediction of parameters by the hydroabrasive machining<sup>5</sup>. The machinability evaluation criterion in almost of all models is a maximum depth of cut  $h$  that can be attained with the given technological parameters. As an alternative the machinability evaluation on the basis of the achieved surface roughness can be used<sup>9</sup>.

Currently, most authors use a model of Zeng and Kim<sup>6</sup>. They have defined the machinability of different materials as a “Machinability Number  $N_M$ ”. On the basis of extensive experimental testing they have determined an empirical formula for calculating the machinability in the form of

$$N_M = \frac{hCD^{0.618}u^{0.866}q}{P_w^{1.25}m_w^{0.687}m^{0.343}} \quad (1)$$

where  $h$  – depth of cut,  $C$  – scale factor of the machinability,  $D$  – focusing tube diameter,  $u$  – cutting speed,  $P_w$  – pressure of water,  $m_w$  – mass flow rate,  $m$  – mass flow rate of abrasive,  $q$  – degree of cut quality<sup>6</sup>.

A level of quality cut  $q$  is chosen in the range of 1 to 5. The value of  $q = 1$  corresponds to the quality of rough cut and the value of  $q = 5$  corresponds to a high surface quality. This model has spread around the world due to its simplicity and many international companies are using this model for optimization of the process parameters in the hydroabrasive machining<sup>1</sup>. A disadvantage of this method of the machinability evaluation is that is based on a subjective quality assessment.

New methodology for the machinability evaluation of materials by the AWJ

A new methodology for the machinability evaluation of materials in the AWJ technology is based on a comparison of a unit volume of material removal.

A newly designed machinability test for the AWJ can be broken down into the following 10 steps:

1. Mass measurement  $m_1$  of tested material with an accuracy of  $\pm 0.01$  g.
2. On the basis of the geometric dimensions of tested sample its volume  $V \pm 5\%$  is determined.
3. Using the equation (2) the density  $\rho$  of material being tested is determined

$$\rho = m_1 / V \quad (2)$$

Note: if the density  $\rho$  is known, the step 2 and 3 can be omitted.

4. On the material being tested a test cut creating a groove in the material is performed. The groove so created is the amount of removed material. When the groove is being created, there must not be cut through the whole thickness of the material. Fig. 1 shows the groove profile created in aluminum alloy.
5. After the groove has been created, it is necessary to dry the sample by airflow. In case of absorbent materials (such as different geomaterials), the sample must be dried in an oven.
6. Measuring of the final mass  $m_2$  of material being tested.
7. Determination of the mass removal rate by the equation (3)

$$\Delta m = m_1 - m_2 \quad (3)$$

8. On the basis of the equation (4) the volume of material removal is determined

$$\Delta V = \Delta m / \rho \quad (4)$$

9. Selection of a unit volume of material removal

$$\Delta V_U = \Delta V / L \quad (5)$$

where  $L$  is a length of the groove being tested.

Note: A unit volume of material removal can be determined by measuring the geometric dimensions of the groove by an optical profilometer. Fig. 1 shows the groove measured by an optical profilometer FRT Micro-Prof.

10. If we know the unit volume of material removal, an in-

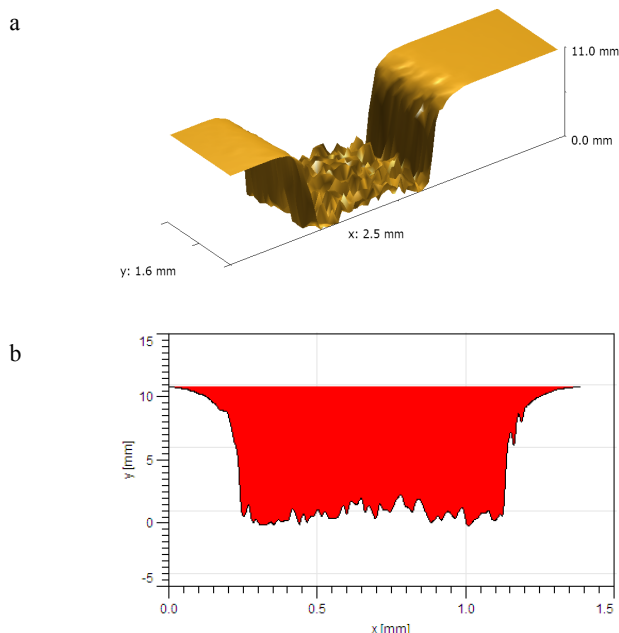


Fig. 1. a) 3D visualization of the groove created by the hydroabrasive machining b) representation of the groove profile

dex of machinability  $M_I$  can be established

$$M_I = \frac{\Delta V_U}{\Delta V_{U_{et}}} \quad (6)$$

where  $\Delta V_{U_{et}}$  is the unit volume of material removal of etalon material.

Note: For materials with the machinability index of less than one, their machinability is worse than the machinability of etalon material. On the contrary, materials with a higher machinability index as one are better for machining than etalon material. Low carbon steel of EN S355J0 was chosen for the etalon material. Given that the different kinds of steel have the machinability index very small, there will be no big mistake, when using of low carbon steel as the etalon material.

### 3. Material and methods

#### Used materials

The experimental part was mainly focused on testing of metallic materials. These were as follows: stainless steel AISI 309, AISI 304 stainless steel, low carbon steel of EN S355J0, pure titanium Grade 2, CuZn40Pb2 brass, aluminum alloy AlMgSi0, 5.

These materials create a group of materials being classified as tough materials. From a group of materials that are known as brittle, was used silicate glass and Silesian granite.

#### Measurement of mechanical properties

In order to understand the machinability of materials by the hydroabrasive machining, it is important to investigate a relationship between the machinability values and physical-mechanical properties of materials. For example we logically consider that the machinability has a relationship with the material hardness. An important parameter is the modulus of elasticity giving information about the elastic behavior of material. The modulus of elasticity shall be usually determined on the basis of the uniaxial tensile test. A suitable alternative to this test is to identify the modulus of elasticity by an instrumented indentation test. The instrumented indentation tests are used for the determination of a wide range of mechanical parameters of material. The most commonly they are used to determine the material hardness. Hardness is described as a material's resistance to entry of foreign particles. Another parameter that can be determined by these tests is the above mentioned modulus of elasticity. The modulus of elasticity is determined from a relief curve.

Microhardness tester from CSM Instruments company was used. A diamond pyramid indenter was used to carry out tests according to Vickers. An advantage of the Vickers test is particularly a low sensitivity of the measured values to a loading force. A maximum loading force of 3000  $\mu\text{N}$  lasting 10 seconds was used in experiments. For each material 10 indentation tests were carried out, from which it was calculated a mean value.

#### 4. Results and discussion

Verification of the newly proposed methodology for the machinability evaluation

To verify accuracy of the obtained results a model of the machinability evaluation proposed by Zeng and Kim was used. Fig. 2 illustrates dependence between the machinability index  $M_I$  and machinability according to Zeng and Kim.

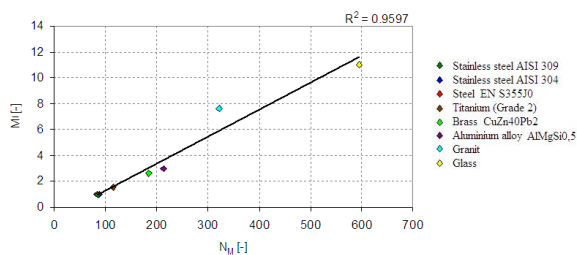


Fig. 2. Dependence of the machinability index  $M_I$  on the machinability parameter  $N_M$

In Fig. 2 it can be seen that the machinability values being determined by the new methodology  $M_I$  are in close agreement with the machinability being determined by Zeng and Kim  $N_M$  (ref. 6).

On the basis of this close agreement it can be determined the correlation equation for the calculation between the two types of machinability may be written

$$N_M = 46.22M_I + 44.56 \quad (7)$$

Use of this relation is very convenient, because the vast majority of devices that are used in a number of companies around the world are programmed to use the parameter of machinability according to Zeng and Kim. The advantage of using the new methodology for the materials machinability evaluation by the AWJ is in that, it can help to eliminate the subjective assessment of surface quality  $q$ . Another advantage is that this method is the least sensitive to a change of the technological parameters during testing.

Effect of mechanical properties on the machinability

If it is possible to find a link between the mechanical properties and machinability of the material, it would be possible to predict the machinability from these properties. This would help to avoid the time-consuming and cost expensive testing of machinability for each material. In Fig. 3 dependence between the observed index of machinability and Vickers hardness  $HV$  is shown.

In Fig. 3 a clear relationship between the material hardness  $HV$  and machinability index  $M_I$  can be seen. Following this it can be concluded that with an increase of the material hardness the machinability of material is being deteriorated. A match between the experimentally measured data and the correlation equation is 89 %.

Fig. 4 shows a relationship between the observed index machinability  $M_I$  and the modulus of elasticity  $E$ .

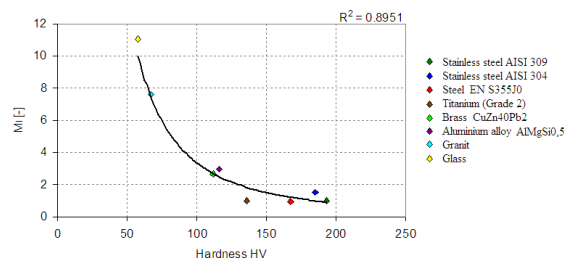


Fig. 3. Relation machinability index  $M_I$  for hardness  $HV$

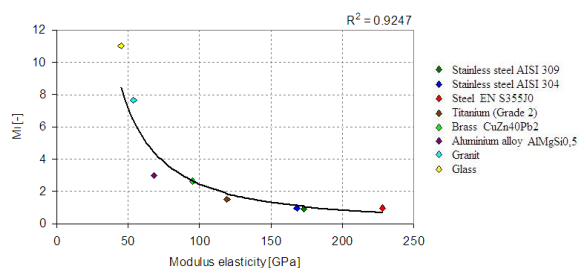


Fig. 4. Relation machinability index  $M_I$  for modulus of elasticity

From Fig. 4 a clear relationship between the index of machinability  $M_R$  and the modulus of elasticity  $E$  can be seen. The correlation coefficient in this case is even higher and thus 92 %.

Proposal of the materials machinability parameter  $M_P$

Given that both the material hardness and the modulus of elasticity are in inverse proportion to the materials machinability, a new materials machinability parameter  $M_P$  has been proposed in equation form of

$$M_P = \frac{E \cdot HV}{E_{et} \cdot HV_{et}} \quad (8)$$

where  $E_{et}$  is the modulus of elasticity of the etalon and  $HV_{et}$  is Vickers hardness of the etalon.

Fig. 5 shows dependence between the machinability index  $M_I$  and the newly materials machinability parameter being proposed.

Fig. 5 shows a good match between the machinability index  $M_I$  and the materials machinability parameter  $M_P$ . The correlation coefficient is close to 99 %.

$$M_I = 0.975M_P^{-1.0484} \quad (9)$$

If the relation (9) is generalized to the equation form (10), we can say that the machinability index  $M_I$  is approximately equal to the inverse value of materials machinability parameter  $M_P$ .

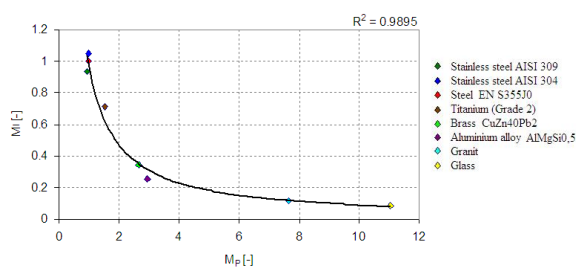


Fig. 5. Dependence of the index of machinability  $M_I$  on the material machinability parameter  $M_P$

$$M_I \cong 1 / M_P \quad (10)$$

## 5. Conclusions

In this paper we propose the new methodology for the machinability evaluation of materials by the hydroabrasive machining, which is based on the comparison of the unit volume of material removal. The advantages of using the new methodology for the machinability evaluation in the AWJ lies in the fact that compared to others methods this method is accurately quantified and there is no subjective assessment of surface quality  $q$ . Another advantage is that this method is the least sensitive to the changes of the technological parameters during testing. It is relatively simple, not expensive and rapid test that requires no special equipment. Verification of the newly proposed methodology was performed by comparing the machinability indexes with the values of machinability according to Zeng and Kim, where a very good match between parameters has been achieved. Therefore the correlation equation for the calculation between the machinability index  $M_I$  and machinability according to Zeng and Kim has been proposed. In this paper the effects of mechanical parameters on the machinability are also evaluated. A clear dependence of the machinability on the material hardness and also on the modulus of elasticity has been proved. The new materials machinability parameter  $M_P$  has been proposed. This parameter can be used to predict the materials machinability in the AWJ technology provided that the modulus of elasticity and Vickers hardness are known.

The work has been supported by projects SGS No. SP/201058, GA ČR No. 101/09/0650, RMTVC No. CZ.1.05/2.1.00/01.0040. Thanks also to the Moravian - Silesian Region for financial support and CEEPUS program CII-PL-0007-05-0910 at the Kielce University of Technology in Poland.

## REFERENCES

1. Liu H. T.: J. of Man. Pro. 12, 8 (2010).
2. Kmeč J., et al.: Technical Gazette 17, 383 (2010).
3. Hassan A. I., et al.: Int. J. of Mach. T. & Man 44, 595 (2004).
4. Meng H., et al.: Wear 181-183, 443 (1995).
5. Hashish M. A.: J. Eng. Mater. Technol. 111, 154 (1989).
6. Zeng J., Kim T.: 7<sup>th</sup> American Water Jet Conference, p. 175–189, USA, Washington 1993.
7. Capello E., Groppeti R.: 7<sup>th</sup> American Water Jet Conference, p. 157–174, USA, Washington 1993.
8. El-Domianty A. A., et al.: Int. J. Adv. Manuf. Tech. 13, 172 (1997).
9. Hlaváček P., et al.: Strojárstvo 51, 273 (2009).

P. Hlaváček<sup>a</sup>, J. Valíček<sup>a</sup>, J. Brumek<sup>b</sup>, M. Zelenák<sup>a</sup>, B. Haluzíková<sup>a</sup>, M. Harničárová<sup>c</sup>, and V. Szarková<sup>d</sup> (<sup>a</sup>Institute of Physics, VŠB-TUO, Czech Republic; <sup>b</sup>SMID - CPIT, VŠB - TUO, Czech Republic; <sup>c</sup>Faculty of Manufac. Technologies of Technical University of Košice with a seat in Prešov, Slovak Republic; <sup>d</sup>Institute of Economics and control systems, VŠB - TUO, Czech Republic): **Use of the Indentation Tests for the Evaluation of Machinability of Materials during Abrasive Waterjet Cutting**

The paper deals with the possibilities of using the indentation tests for the evaluation of machinability of materials during abrasive water jet cutting. Indentation tests are used to simulate the interaction between abrasive particles and material during the process of abrasive water jet cutting. On the basis of these tests the machinability of materials can be characterized. The machinability of materials is very important for optimization of the technological process parameters of abrasive water jet cutting, which affect the quality, performance and economy of the entire process.